

Analytic Skyrmionic crystals in the Skyrme model in (3+1) dimensions at finite density and fractional Baryonic charge

Fabrizio Canfora¹

¹*Centro de Estudios Científicos (CECS), Casilla 1469, Valdivia, Chile.*

canfora@cecs.cl

September 2, 2022

Abstract

Different types of numerical approximations of cold dense nuclear matter suggested that baryons in such a regime should be in a solid crystalline phase. Here the first analytic solutions in the (3+1)-dimensional Skyrme model representing multi-layered configurations of Skyrmions with crystalline structure living in flat space-times at finite density are presented. The number of the peaks in the energy density in each layer is related with the Baryonic charge of that layer. The positions of the peaks in each layer can be computed explicitly by maximizing the energy density and they manifest a clear crystalline order. The total Baryon charge is the product of the number of layers times the Baryon charge of the layers. This construction provides with the first exact description of the so-called popcorn transitions in the low energy limit of full-fledged QCD. The present construction reveals the intriguing possibility of fractional Baryonic charges as the bumps in these crystal-like structures carry a fraction of $1/q$ of unit Baryonic charge (q being an odd integer). The propagation of electrons (Fermions) in these crystalline structures confirms the presence of fractional Baryonic charges.

1 Introduction

One of the main open problems in high energy physics is to understand the phases of cold and dense nuclear matter as a function of baryon number density [1] [2]. The theoretical dream would be to derive analytically (using the low energy limit of QCD) the appearance of crystals-like structures in Baryonic matter at finite density. One could think that this task is far beyond the reach of the available theoretical tools. Until quite recently, the only theoretical arguments supporting the appearance of Baryonic crystals at finite density could be found in two-dimensional effective toy models (see [3], [4] and references therein). This situation has led to a number of different approximate descriptions to describe this phase.

From the theoretical point of view, a very interesting approximation (based on the AdS/CFT correspondence [5]) which has been widely used has been proposed in [6] [7] [8] [9]. Within this framework, a significant difficulty is to calculate the required solitons: only single baryon solutions have

been discussed in details [10] [11]. Hence, numerical solutions at finite density in full Sakai-Sugimoto model are extremely difficult (see [12] [13]). Even when one considers low-dimensional analogues of the setting in [6], multi-baryons at finite density must be necessarily analyzed numerically.

Despite all the above difficulties, it has been argued that baryons in such a regime *are necessarily in a solid crystalline phase* [8]. Another prediction based on the above numerical results is that a series of phase transitions (called *popcorn transitions*) are expected when the Baryon density is increased. Tractable numerical analysis are available in (2+1) dimensions (see in particular [14] [15] [16]).

An explicit analytic approach to the two predictions above in the context of the low energy limit of (3+1)-dimensional QCD is the main goal of the present paper.

The Skyrme theory represents such low energy limit [17] (for detailed reviews on Skyrme theory see [18] [19]). Its topological solitons (called Skyrmions) represent Baryons (see [20] [21] and references therein). The wide range of applications of this theory in many different fields (see [23], [24], [25], [26], [27] and references therein) is well recognized.

The appearance of crystal-like structures in the Skyrme model is well established numerically (see [19] [22] and references therein). Within the rational map approach [22] one can construct numerically configurations in which the number of "bumps" in the energy density is related with the corresponding Baryon charge.

Due to the above arguments, one may argue that, in the Skyrme model (which represents the low energy limit of full-fledged QCD), to construct exact analytic multi-Skyrmionic solutions with crystal-like structures at finite density is almost impossible.

In fact, the generalized hedgehog ansatz introduced in [28] [29] [30] [31] [32] [33] [34] [35] allowed the construction of the first analytic multi-Skyrmions at finite density (however, these Skyrmions at finite density do not have crystal-like structure).

In the present paper, the methods in [34] [35] will be generalized to construct multi-layered configurations of Skyrmions in such a way that each layer has a crystal structures in which the number of peaks of the energy density is related with the Baryon number in each layer and the layer can pile up along the third flat directions. One then observes transitions in which for fixed total topological charge, configurations with more layers but lower densities are energetically favored over configurations made of a smaller number of layers but with higher densities. A quite remarkable possibility disclosed by the present construction is that, within these structures, topological excitations with fractional Baryonic charge may appear.

This paper is organized as follows: in the second section the Skyrme model is introduced and the Skyrme field equations are written in two equivalent ways: this is very important in order to check that the present crystals are really solutions of the full Skyrme field equations. In the third section, the method to go beyond the spherical hedgehog ansatz is introduced and the analytic multi-layers crystal-like Skyrmions are derived. In the fourth section, some properties of electrons propagating in this Baryonic environment are analyzed. In the final section, some conclusions will be drawn.

2 Skyrme model beyond the hedgehog

The first analytic tool to construct multi-Skyrmionic crystal-like configurations which generalizes the finite density approach in [34] [35] will be described. The action of the $SU(2)$ Skyrme system is

$$S_{Sk} = \frac{K}{2} \int d^4x \sqrt{-g} \text{Tr} \left(\frac{1}{2} L^\mu L_\mu + \frac{\lambda}{16} F_{\mu\nu} F^{\mu\nu} \right) \quad K > 0, \quad \lambda > 0, \quad (1)$$

$$L_\mu := U^{-1} \nabla_\mu U = L_\mu^j t_j, \quad F_{\mu\nu} := [L_\mu, L_\nu], \quad \hbar = 1, \quad c = 1,$$

where K and λ are the coupling constants¹, $\mathbf{1}_2$ is the 2×2 identity matrix and the t^j are the basis of the $SU(2)$ generators (where the Latin index j corresponds to the group index).

The three coupled Skyrme field equations are

$$\nabla^\mu L_\mu + \frac{\lambda}{4} \nabla^\mu [L^\nu, F_{\mu\nu}] = E^j t_j = 0, \quad j = 1, 2, 3. \quad (2)$$

while the energy density (the $0 - 0$ component of the energy-momentum tensor) reads

$$T_{00} = -\frac{K}{2} \text{Tr} \left[L_0 L_0 - \frac{1}{2} g_{00} L^\alpha L_\alpha + \frac{\lambda}{4} \left(g^{\alpha\beta} F_{0\alpha} F_{0\beta} - \frac{g_{00}}{4} F_{\sigma\rho} F^{\sigma\rho} \right) \right]. \quad (3)$$

The following parametrization of the $SU(2)$ -valued scalar $U(x^\mu)$ will be adopted

$$U^{\pm 1}(x^\mu) = \cos(\alpha) \mathbf{1}_2 \pm \sin(\alpha) n^i t_i, \quad n^i n_i = 1, \quad (4)$$

$$n^1 = \sin F \cos G, \quad n^2 = \sin F \sin G, \quad n^3 = \cos F. \quad (5)$$

Thus, the $SU(2)$ Skyrme action in (3+1)-dimensions describes the non-linear interactions between three degrees of freedom (namely, α , F and G) which parametrize the most general $SU(2)$ element. In general α , F and G are functions of the four space-time coordinates. The main technical problem is to find a good ansatz which keeps alive the non-trivial topological charge and, at the same time, allows for a crystal-like structure in the energy density without making the field equations impossible to solve analytically (this point will be discussed in the next subsection). It is worth to note that with the usual hedgehog ansatz in [17] (as well as in its finite density generalization [34] [35]) the energy density in Eq. (3) (due to the trace on the internal indices) only depends on the Skyrmion profile.

The Baryon charge of the configuration reads

$$W = B = \frac{1}{24\pi^2} \int_{\{t=const\}} \rho_B, \quad (6)$$

$$\rho_B = \epsilon^{ijk} \text{Tr} (U^{-1} \partial_i U) (U^{-1} \partial_j U) (U^{-1} \partial_k U). \quad (7)$$

¹They can be determined as in [21].

In terms of α , F and G , the topological density ρ_B reads

$$\rho_B = 12 (\sin^2 \alpha \sin F) d\alpha \wedge dF \wedge dG . \quad (8)$$

2.1 Explicit parametrization

It is useful to write down the Skyrme field equations explicitly in terms of the three scalar degrees of freedom α , F and G . In this way, it is possible to check directly that the ansatz proposed in the following sections is consistent. It is useful to introduce the following functions $Y^0(x^\mu)$ and $Y^i(x^\mu)$

$$\begin{aligned} Y^0 &= \cos \alpha, \quad Y^1 = \sin(\alpha) \sin(F) \cos(G), \\ Y^2 &= \sin(\alpha) \sin(F) \sin(G), \quad Y^3 = \sin(\alpha) \cos(F) . \end{aligned} \quad (9)$$

In this way, the most general element U of $SU(2)$ can be written as

$$U = \mathbf{I}Y^0 + Y^i t_i \quad ; \quad U^{-1} = \mathbf{I}Y^0 - Y^i t_i .$$

These functions are useful to write down the Skyrme action explicitly in terms of α , F and G . Introducing the tensor $\Sigma_{\mu\nu}$

$$\Sigma_{\mu\nu} = G_{ij} \nabla_\mu Y^i \nabla_\nu Y^j \quad ; \quad G_{ij} = \delta_{ij} + \frac{Y^i Y^j}{1 - Y^k Y_k} \quad (10)$$

the Skyrme action is then defined as

$$I = \int d^4x \sqrt{-g} \left[\frac{1}{2} \Sigma^\mu_\mu + \frac{\lambda}{4} ((\Sigma^\mu_\mu)^2 - \Sigma^{\mu\nu} \Sigma_{\mu\nu}) \right] . \quad (11)$$

Now, we are in the position to write down the general Skyrme field equations in terms of α , F and G . The variation of the Skyrme action with respect to α leads to the equation of motion

$$+ \lambda \left(\begin{array}{l} (-\square \alpha + \sin(\alpha) \cos(\alpha) (\nabla_\mu F \nabla^\mu F + \sin^2 F \nabla_\mu G \nabla^\mu G)) \\ \sin(\alpha) \cos(\alpha) ((\nabla_\mu \alpha \nabla^\mu \alpha) (\nabla_\nu F \nabla^\nu F) - (\nabla_\mu \alpha \nabla^\mu F)^2) \\ + \sin(\alpha) \cos(\alpha) \sin^2(F) ((\nabla_\mu \alpha \nabla^\mu \alpha) (\nabla_\nu G \nabla^\nu G) - (\nabla_\mu \alpha \nabla^\mu G)^2) \\ + 2 \sin^3(\alpha) \cos(\alpha) \sin^2(F) ((\nabla_\mu F \nabla^\mu F) (\nabla_\nu G \nabla^\nu G) - (\nabla_\mu F \nabla^\mu G)^2) \\ - \nabla_\mu (\sin^2(\alpha) (\nabla_\nu F \nabla^\nu F) \nabla^\mu \alpha) + \nabla_\mu (\sin^2(\alpha) (\nabla_\nu \alpha \nabla^\nu F) \nabla^\mu F) \\ - \nabla_\mu (\sin^2(\alpha) \sin^2(F) (\nabla_\nu G \nabla^\nu G) \nabla^\mu \alpha) + \nabla_\mu (\sin^2(\alpha) \sin^2(F) (\nabla_\nu \alpha \nabla^\nu G) \nabla^\mu G) \end{array} \right) = 0 , \quad (12)$$

The variation of the Skyrme action with respect to F leads to the equation of motion

$$+ \lambda \left(\begin{array}{l} (-\sin^2(\alpha)\square F - 2\sin(\alpha)\cos(\alpha)\nabla_\mu\alpha\nabla^\mu F + \sin^2(\alpha)\sin(F)\cos(F)\nabla_\mu G\nabla^\mu G) \\ \sin^2(\alpha)\sin(F)\cos(F)((\nabla_\mu\alpha\nabla^\mu\alpha)(\nabla_\nu G\nabla^\nu G) - (\nabla_\mu\alpha\nabla^\mu G)^2) \\ + \sin^4(\alpha)\sin(F)\cos(F)((\nabla_\mu F\nabla^\mu F)(\nabla_\nu G\nabla^\nu G) - (\nabla_\mu F\nabla^\mu G)^2) \\ - \nabla_\mu(\sin^2(\alpha)(\nabla_\nu\alpha\nabla^\nu\alpha)\nabla^\mu F) + \nabla_\mu(\sin^2(\alpha)(\nabla_\nu\alpha\nabla^\nu F)\nabla^\mu\alpha) \\ - \nabla_\mu(\sin^4(\alpha)\sin^2(F)(\nabla_\nu G\nabla^\nu G)\nabla^\mu F) + \nabla_\mu(\sin^4(\alpha)\sin^2(F)(\nabla_\nu F\nabla^\nu G)\nabla^\mu G) \end{array} \right) = 0, \quad (13)$$

The variation of the Skyrme action with respect to G leads to the equation of motion

$$(-\sin^2(\alpha)\sin^2(F)\square G - 2\sin(\alpha)\cos(\alpha)\sin^2(F)\nabla_\mu\alpha\nabla^\mu G - 2\sin^2(\alpha)\sin(F)\cos(F)\nabla_\mu F\nabla^\mu G) \\ + \lambda \left(\begin{array}{l} -\nabla_\mu[\sin^2(\alpha)\sin^2(F)(\nabla_\nu\alpha\nabla^\nu\alpha)\nabla^\mu G] + \nabla_\mu[\sin^2(\alpha)\sin^2(F)(\nabla_\nu\alpha\nabla^\nu G)\nabla^\mu\alpha] \\ -\nabla_\mu[\sin^4(\alpha)\sin^2(F)(\nabla_\nu F\nabla^\nu F)\nabla^\mu G] + \nabla_\mu[\sin^4(\alpha)\sin^2(F)(\nabla_\nu F\nabla^\nu G)\nabla^\mu F] \end{array} \right) = 0. \quad (14)$$

2.1.1 Example: the original Skyrme ansatz

Here we give a simple examples showing that the above equations (12), (13) and (14). The original Skyrme ansatz is defined by the choice

$$\alpha = \alpha_s(r), \quad F = \theta, \quad G = \varphi, \quad (15)$$

in the following flat metric in spherical coordinates:

$$ds^2 = g_{\mu\nu}dx^\mu dx^\nu = -dt^2 + dr^2 + r^2(d\theta^2 + \sin\theta^2 d\varphi^2). \quad (16)$$

One can check that, due to the identities

$$\nabla_\mu\alpha_s\nabla^\mu F = \nabla_\mu G\nabla^\mu\alpha_s = \nabla_\mu G\nabla^\mu F = 0, \quad (17)$$

and to the fact that both F and G are linear functions in the chosen coordinates system, the three Skyrme field equations (12), (13) and (14) reduce to only one consistent scalar equation for the profile $\alpha_s(r)$. A crucial technical detail is the following: in the equation for $\alpha_s(r)$ (namely, Eq. (12)) potentially dangerous terms are the ones involving $\sin F^2$ as these terms involve θ while one would like to have a consistent equation for $\alpha_s(r)$ which, therefore, only involves r dependence. In the original ansatz of Skyrme the dangerous θ -dependence due to $\sin F^2$ is canceled by the inverse metric $g^{\varphi\varphi}$ appearing in $\nabla_\mu G\nabla^\mu G$. Thus, one can reduce the three Skyrme field equations to a single scalar equation for $\alpha_s(r)$. In particular, if one plugs the ansatz in Eq. (15) into the three Skyrme field equations (12), (13) and (14) one can see directly that Eqs. (13) and (14) are identically satisfied and that Eq. (12) reduces to the usual equation for the Skyrme profile $\alpha_s(r)$ which can be found in all the textbooks (see, for instance, [19]). In the following, a different trick to get a consistent equation for α in a topologically non-trivial sector will be introduced.

3 Skyrme Crystals

The main physical motivation of the present work is to study finite density effects. The easiest way to take into account finite-density effects is to introduce the following flat metric

$$ds^2 = -dt^2 + A(dr^2 + d\theta^2) + L^2 d\phi^2 , \quad (18)$$

where $2\pi L$ is the size of the box in the direction orthogonal to the crystal layers while $2\pi^2 A$ is area of the layers. The adimensional coordinates r , θ and ϕ have the periods

$$0 \leq r \leq 2\pi , \quad 0 \leq \theta \leq \pi , \quad 0 \leq \phi \leq 2\pi . \quad (19)$$

Following the strategy of [34] [35], the boundary conditions in the θ direction here will be chosen to be Dirichlet while in the r and ϕ directions they can be both periodic and anti-periodic.

The ansatz for the multi-layered Skyrme crystal is

$$\alpha = \alpha(r) , \quad F = q\theta , \quad G = p\left(\frac{t}{L} - \phi\right) , \quad q = 2v + 1 , \quad p, v \in \mathbb{N} , \quad p \neq 0 . \quad (20)$$

With the above ansatz the topological density in Eq. (7) reads

$$\rho_B = (12pq \sin(q\theta) \sin^2 \alpha) \partial_r \alpha . \quad (21)$$

The boundary condition on α and the corresponding Baryon charge are

$$\alpha(2\pi) - \alpha(0) = n\pi \Rightarrow B = np . \quad (22)$$

A useful way to think at the Baryon B number in the present case is the following: one first integrates the topological density in Eq. (21) (multiplied by the normalization factor $1/24\pi^2$) corresponding to the Skyrmionic configuration in Eq. (20) along the ϕ direction (which, in a sense, is the less interesting direction as neither the topological density nor the energy density-see Eq. (32) below-depend on ϕ) which gives an extra factor of 2π . In this way, one obtains an effective two-dimensional topological density σ_B which, when integrated in r and θ , gives the total Baryon charge of the configuration:

$$\sigma_B = \frac{1}{24\pi^2} \int_0^{2\pi} \rho_B d\phi = \frac{(pq \sin(q\theta) \sin^2 \alpha)}{\pi} \partial_r \alpha , \quad (23)$$

$$B = \int \sigma_B dr d\theta . \quad (24)$$

Thus, one can think at σ_B as the effective topological density of the layers which is obtained integrating the topological density ρ_B in Eqs. (7) and (21) along the ϕ direction.

When one plugs the ansatz in Eq. (20) into the three coupled Skyrme field equations in Eq. (2),

they reduce to only one integrable equation for $\alpha(r)$:

$$E_j = c_j P[\alpha] , \quad c_j \neq 0 , \quad j = 1, 2, 3, \quad (25)$$

$$P[\alpha] = 0 \Leftrightarrow \partial_r \left[Y(\alpha) \frac{(\partial_r \alpha)^2}{2} - V(\alpha) - E_0 \right] = 0 , \quad (26)$$

$$Y(\alpha) = (A + q^2 \lambda \sin^2 \alpha) , \quad V(\alpha) = \frac{q^2 A}{2} \sin^2 \alpha \Rightarrow$$

$$\eta(\alpha, E_0) \stackrel{\text{def}}{=} \frac{[2(E_0 + V(\alpha))]^{1/2}}{Y(\alpha)^{1/2}} \Rightarrow \quad (27)$$

$$\frac{d\alpha}{\eta(\alpha, E_0)} = dr , \quad (28)$$

where E_0 is an integration constant to be fixed requiring the boundary condition² in Eq. (22).

An alternative way to see that the above ansatz reduce the full Skyrme field equations to just one equation for the profile α is to use the explicit parametrization of the Skyrme action in term of α , F and G in Eqs. (9), (10) and (11). In this way, one can read directly the field equations for the three functions α , F and G . The relevant properties of the ansatz in Eq. (20) are

$$\nabla_\mu \alpha \nabla^\mu F = \nabla_\mu \alpha \nabla^\mu G = \nabla_\mu G \nabla^\mu F = 0 , \quad (29)$$

$$\nabla_\mu G \nabla^\mu G = 0 . \quad (30)$$

If one takes into account Eqs. (29) and (30) together with the fact that both F and G depend linearly on the coordinates, one can see easily that Eqs. (13) and (14) are identically satisfied and that Eq. (12) reduces to Eq. (26). Thus, unlike what happens in the case of the original Skyrme ansatz discussed in the previous section, in the present case one can reduce the three Skyrme field equations to only one consistent equation for $\alpha(r)$ because the potentially dangerous terms involving $\sin F$ appearing in Eq. (12) are eliminated by the property in Eq. (30).

Thus, the three coupled Skyrme field equations Eq. (2) with the ansatz in Eq. (20) reduce to a simple quadrature which can be integrated using elliptic functions. The boundary condition in Eq. (22) reduces to:

$$\int_0^{n\pi} \frac{d\alpha}{\eta(\alpha, E_0)} = n \int_0^\pi \frac{d\alpha}{\eta(\alpha, E_0)} = 2\pi , \quad E_0 > 0 . \quad (31)$$

The above equation for E_0 always has a positive real solution³. Moreover, one can see that $\partial_r \alpha > 0$ and that, when n is large, both $\eta(\alpha, E_0)$ and E_0 are of order n .

The energy density (replacing $(\partial_r \alpha)^2$ with $\eta(\alpha, E_0)^2$ using Eq. (27)) in Eq. (3) with the ansatz in

²The positive sign of the square root of $(\partial_r \alpha)^2$ has been chosen.

³The left hand side of Eq. (31) as function of E_0 increases from very small values (when E_0 is very large and positive) to very large values (when E_0 is close to zero but positive). Thus, there is always a value of E_0 which satisfies Eq. (31).

Eq. (20) reads

$$T_{00} = \frac{Kp}{4L^2A} [2\rho_0(\alpha) + 4\sin^2(q\theta)\rho_1(\alpha)] , \quad (32)$$

where

$$\rho_0(\alpha) = \frac{(Lq)^2}{p} \sin^2 \alpha + \eta(\alpha, E_0)^2 \left[\frac{(L)^2}{p} + \lambda \frac{(Lq)^2}{Ap} \sin^2 \alpha \right] , \quad (33)$$

$$\rho_1(\alpha) = \sin^2 \alpha \left[Ap + \lambda q^2 p \sin^2 \alpha + \lambda p \eta(\alpha, E_0)^2 \right] . \quad (34)$$

There are two important differences with respect to the first analytic examples of Skyrmions living at finite density in flat spaces [34] [35]. *Firstly*, in that references, the factor $\sin 2H$ (where H is the profile defined in Eqs. (9) and (10) of [34]) appears linearly in the Baryon density in Eq. (16) of [34]. Thus, in that references, it is not possible to increase the Baryon charge by increasing the number of "bumps" in the profile H . *Secondly*, the energy density (defined in Eq. (15) of [34]) only depends on H (and, consequently, it only depends on one spatial coordinate). This prevents one from describing explicitly crystal-like structures in which the number of bumps in the energy-density is related with the Baryon number (as, in that references, only one bump in H is allowed).

In the present case both problems are solved since in the Baryon density in Eq. (21) $\sin \alpha$ appears quadratically (so that by increasing the number of "bumps" in α one also increases the Baryon charge) and the *energy density in Eqs. (32), (33) and (34) (even after taking the trace over the $SU(2)$ indices) depends non-trivially both on the profile α and on the spatial coordinate θ* (so that a clear crystal-like structure in its peaks emerges).

The two contour plots below (with $p = 1$, $q = 1$ and $n = 25$ on the left and $p = 1$, $q = 3$ and $n = 25$ on the right) of the energy-density as function of α and θ (note that one can replace the r -dependence with the α -dependence in the energy density using Eq. (27) to eliminate dr and $\partial_r \alpha$ in favour of $d\alpha$ and $\eta(\alpha, E_0)$) show the crystal-like pattern of the bumps (whose positions can be determined explicitly maximizing the energy-density):

Thus, these configurations are multi-layered Skyrmions crystals made up by p layers along the ϕ direction with n Skyrmions in each layer.

The total energy E_{tot} of the configuration can be obtained in a closed form (using Eqs. (27) and (28)). One is left with an integral of an explicitly known function of α which contains all the relevant informations:

$$E_{tot} = \int \sqrt{-g} d^3x T_{00} = B\pi^2 K \int_0^\pi d\alpha \Omega(\alpha; p, q, n) , \quad (35)$$

$$\begin{aligned} \Omega(\alpha; p, q, n) = & \frac{A \sin^2 \alpha}{\eta(\alpha, E_0)} \left[\frac{Lq^2}{Ap} + \frac{p}{L} + \frac{\lambda pq^2}{AL} \sin^2 \alpha \right] + \\ & + \frac{\eta(\alpha, E_0)}{A} \left[\frac{AL}{p} + \lambda \sin^2 \alpha \left(\frac{Lq^2}{p} + \frac{Ap}{L} \right) \right] , \end{aligned} \quad (36)$$

where $B = np$ is the Baryon number, n is the number of bumps associated with the profile α in the r direction and p is the number of layers. The special role of the integer q will be discussed in the next

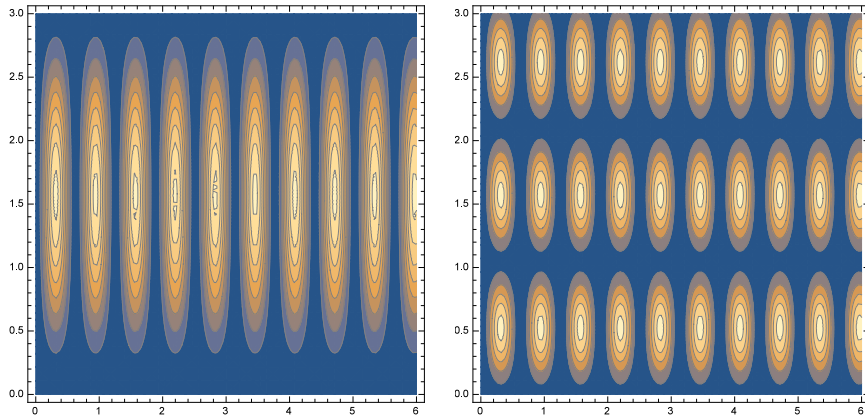


Figure 1: The left panel (a) shows the contour plot of the energy density with $p = 1$, $n = 25$ and $q = 1$ (where the highest energy density is in clear yellow while the lowest is blue). The right panel (b) shows the contour plot of the energy with $p = 1$, $n = 25$ and $q = 3$ (in both cases it has been assumed that $K = 2$ and $\lambda = 1$; note that the horizontal axis corresponds to the r direction while the vertical axis to the θ direction). The patterns of the peaks clearly show a crystal-like structure. It is clear to see that, when passing from $q = 1$ to higher values of q (keeping fixed n and p), the bumps in the energy density (which, when $q = 1$, carry one unit of Baryon charge) are divided into q smaller bumps each of which carries $1/q$ of Baryon charge.

section. The above equation represents the explicit expression for the total energy of the system as a function of the parameters of the system.

A natural question is [7] [8] [9] [14] [15] [16]:

given a total Baryon number B , is it energetically more convenient to have higher p and lower n or the other way around?

In those references, it is argued using different type of numerical approximations that with increasing density a series of transitions takes place where the solitons crystal develops additional layers in the direction orthogonal to the layers. Here it is possible to answer directly to this answer in the low energy limit of full-fledged QCD just by looking at the function $\Omega(\alpha; p, q, n)$ defined in Eq. (36) which contains all the relevant informations. For instance, one can see explicitly that if A decreases (which means increasing the Baryon density of the layers) it is better to have larger values for p (namely, to increase the number of layer). On the other hand, if one increases p it is better to increase L in such a way to keep p/L constant⁴.

3.1 A remark on the stability

A remark on the stability of the above crystals is in order. When the hedgehog property holds (so that the field equations reduce to a single equation for the profile) the most dangerous perturbations are perturbations of the profile which keep the structure of the ansatz (see [36] [37] and references

⁴A complete study of $\Omega(\alpha; p, q, n)$ is beyond the scope of the present paper. Anyway, the total energy can be obtained in a closed form in terms of elliptic integrals. I hope to come back on a complete analysis of $\Omega(\alpha; p, q, n)$ and of its integral in a future publication.

therein). In the present case these are

$$\alpha \rightarrow \alpha + \varepsilon u(r) , \quad \varepsilon \ll 1 . \quad (37)$$

It is a direct computation to show that the linearized version of Eq. (26) around a background solution $\alpha_0(r)$ of charge $B = np$ always has the following zero-mode: $u(r) = \partial_r \alpha_0(r)$. Due to Eqs. (27), (28) and (31) $u(r)$ has no node so that it must be the perturbation with lowest energy. Thus, the present solutions are stable under the above perturbations. It is also worth to remark that isospin modes $U^A = A^{-1}U_0A$ (where U_0 is the solution of interest and A is a generic $SU(2)$ matrix which only depends on time) have positive energies (if the energy of U_0 is positive, as in the present case) [21]. The effective action for these modes is the one of a spinning top and the energy of the corresponding perturbations is positive definite. Isospin modes are "transverse" to the perturbations of the profile in Eq. (37) as they do not touch $\alpha(r)$: the reason is that both $U^A = A^{-1}U_0A$ and U_0 have the same profile.

This stability argument (which holds for any n, p and q in Eqs. (4), (5), (20) and (22)) in favor of stability is non-trivial. For instance, in the original spherical ansatz of Skyrme with radial profile α_s discussed in the previous sections, the topological density is also proportional to $\sin^2 \alpha_s$ so that one can increase the winding increasing the "spherical bumps" in the energy density (which in the case of the original spherical ansatz of Skyrme only depends on the radius). As it is well known, one can construct (numerically) these "higher charges spherical Skyrmions" but all of them are unstable. The instability (which cannot arise from the "Isospin modes" discussed above) arises from zero modes of the form $\partial_r \alpha_s$ with nodes (so that there are perturbations with negative energies and, indeed, the only stable solution of this family is the spherical Skyrmion of charge 1).

4 Bumps with fractional Baryonic charge

The crystal-like structures constructed in the previous section are characterized by three integers: p, n and q . The role of the odd-integer q (which does not enter directly in the Baryon charge in Eq. (22)) has not been discussed. A clear hint is the comparison of the energy-density contour plots above for two such crystal-like structures with the same Baryon charges, p and n but different q (for instance, $p = 1, q = 1$ and $q = 3$). As it is clear from these plots, there are n bumps in the first structure with $q = 1$ which correspond exactly to the Baryon charge of the layers: thus, each bump carries one unit Baryon charge as expected (this can be easily computed integrating the effective two-dimensional topological density σ_B in Eqs. (23) and (24) over the $r - \theta$ area occupied by the elementary bump). In the second structure with $q = 3$ there are $3n$ bumps but the Baryon charge has not changed. Thus, each bump carries $1/3$ (in general $1/q$) of the unit topological charge (also this can be confirmed computing integrating the topological density over the $r - \theta$ -area occupied by the "fractional" bump). This is a very intriguing phenomenon as, usually, the appearance of "fractional charges" is associated with condensed matter physics (and, in particular, to the Fractional Quantum Hall Effect) while it is a completely unexpected phenomenon in the low energy limit of QCD. Thus, the integer q is related

to the fractional Baryonic charge carried by the bumps of the crystal.

The transport properties of electrons (Fermions) through these Skyrmionic crystals disclose the relevance of these fractional bumps. At semi-classical level, these are determined by the corresponding Dirac equation. The interactions of the electrons with the Baryonic background can be described as “current-current” interactions:

$$H_{int}^B = g_{eff} J_\mu^e J_\mu^B, \quad g_{eff} \approx G_F, \\ J_\mu^e = \bar{\Psi} \gamma_\mu \Psi, \quad J_\mu^B = \frac{\sqrt{-g} \epsilon_{\mu\alpha\beta\nu}}{24\pi^2} \text{Tr} \left(L^\alpha L^\beta L^\nu \right),$$

where J_μ^B is the Baryonic current associated to the above Skyrmionic crystals, $J_0^B = \rho_B$ is the topological density in Eq. (21), γ_μ are the Dirac gamma-matrices. At the present level of approximation (in which the energy scale of the Fermion is not high enough to disclose the parton structure of the Baryon) g_{eff} is basically the electro-weak Fermi constant $G_F \sim 1.166 \text{ GeV}^{-2}$. Similar results should be expected for any Fermion propagating in this Baryonic environment (changing g_{eff} accordingly).

The Dirac equation describing the propagation of the electron through the above Skyrmions crystals is

$$\left[\gamma^\mu \left(i \nabla_\mu - \tilde{A}_\mu \right) + m \right] \Psi = 0, \quad \tilde{A}_\mu = G_F J_\mu^B \quad (38)$$

where m is the electron mass. Even without an explicit solution, one can argue that the corresponding spectrum will present energy bands for spinor wave functions of the form $\Psi = \exp(-i(Et - k_3\phi)) \psi(r, \theta)$. The spinor Ψ perceives J_μ^B as an effective gauge potential \tilde{A}_μ which depends periodically on r and θ : thus, the Bloch theorem applies. The topological density ρ_B in Eq. (21) plays the role of an effective electric potential. It is easy to see that, when $q \neq 1$, the area of the “valleys” of the electric potential coincide with the area of the bumps in the energy-density carrying fractional Baryonic charge mentioned above. Consequently, the electrons (Fermions) feel directly the presence of fractional Baryonic charge. Also the band spectrum of Eq. (38) is determined by the spacing between the fractional bumps. Hence, at least in principle, one can measure directly these fractional Baryonic bumps analyzing these transport properties.

5 Conclusions

The first analytic multi-layered configurations of Skyrmions with crystalline structure living in flat space-times at finite density have been presented. These configurations are characterized by three integers: n , p and q (q being an odd integer). The Baryonic charge of the layers is n while p is the number of layers so that the total Baryonic charge is $B = np$. Remarkably, when $q \neq 1$, the bumps in these crystal-like structures carry a fraction of $1/q$ of Baryonic charge. The positions of the peaks in the energy-density in each layer can be computed explicitly by maximizing the energy density. This construction provides with the first exact analytic description of the so-called popcorn transitions in the low energy limit of full-fledged QCD. The transport properties of Fermions in these structures allow, in principle, to detect the presence of fractional Baryonic charges. The present results greatly

enlarge the phenomenological applications of the Skyrme model.

Acknowledgements

This work has been funded by the Fondecyt grants 1160137. The author would like to thank C. Martinez for useful suggestions. The Centro de Estudios Científicos (CECs) is funded by the Chilean Government through the Centers of Excellence Base Financing Program of Conicyt.

References

- [1] P. de Forcrand, *Simulating QCD at finite density*, PoS(LAT2009)010 [arXiv:1005.0539] [INSPIRE].
- [2] N. Brambilla et al., QCD and Strongly Coupled Gauge Theories: Challenges and Perspectives, Eur. Phys. J. C 74 (2014) 2981 [arXiv:1404.3723] [INSPIRE].
- [3] K. Takayama, M. Oka, *Nucl. Phys. A* **551** (1993), 637-656.
- [4] V. Schön, M. Thies, *Phys. Rev. D* **62** (2000) 096002.
- [5] J. Maldacena, *Advances in Theoretical and Mathematical Physics* **2**: 231–252, (1998).
- [6] T. Sakai and S. Sugimoto, *Prog. Theor. Phys.* **113**, 843 (2005).
- [7] M. Rho, S. -J. Sin, I. Zahed, *Phys. Lett. B* 689 (2010) 23.
- [8] V. Kaplunovsky, D. Melnikov, J. Sonnenschein, JHEP 1211 (2012) 047; *Modern Physics Letters B* **29**, No. 16 (2015) 1540052.
- [9] V. Kaplunovsky and J. Sonnenschein, JHEP 1404 (2014) 022.
- [10] M. Elliot-Ripley, P. Sutcliffe, M. Zamaklar, JHEP 1610, 88 (2016).
- [11] S. Bolognesi, P. Sutcliffe, JHEP 1401 (2014) 078.
- [12] F. Preisa, A. Schmitt, JHEP 07 (2016) 001.
- [13] P. Sutcliffe, *Modern Physics Letters B* **29**, (2015) 1540051.
- [14] S. Bolognesi, P. Sutcliffe, J.Phys. A47 (2014) 135401.
- [15] M. Elliot-Ripley, T. Winyard, JHEP 1509 (2015) 009.
- [16] M. Elliot-Ripley, J. Phys. A **50**, no. 14, 145401 (2017).
- [17] T. Skyrme, *Proc. R. Soc. London A* **260**, 127 (1961); *Proc. R. Soc. London A* **262**, 237 (1961); *Nucl. Phys.* **31**, 556 (1962).

- [18] H. Weigel, *Chiral Soliton Models for Baryons*, (Springer Lecture Notes 743)
- [19] N. Manton and P. Sutcliffe, *Topological Solitons*, (Cambridge University Press, Cambridge, 2007).
- [20] A.P. Balachandran, A. Barducci, F. Lizzi, V.G.J. Rodgers, A. Stern, *Phys. Rev. Lett.* **52** (1984), 887.
- [21] G. S. Adkins, C. R. Nappi, E. Witten, *Nucl. Phys.* **B 228** (1983), 552-566.
- [22] C. J. Houghton, N. S. Manton, P. M. Sutcliffe, *Nucl. Phys.* **B 510**, 507 (1998).
- [23] J.-I. Fukuda, S. Zumer, *Nature Communications* **2** (2011), 246.
- [24] Christian Pfleiderer, Achim Rosch, *Nature* **465**, 880–881 (2010).
- [25] S. Seki, X. Z. Yu, S. Ishiwata, Y. Tokura, *Science* **336** (2012), pp. 198-201.
- [26] U. K. Roessler, A. N. Bogdanov, C. Pfleiderer, *Nature* **442**, 797 (2006).
- [27] A. N. Bogdanov D. A. Yablonsky, *Sov. Phys. JETP* **68**, 101 (1989).
- [28] F. Canfora, *Phys. Rev.* **D 88**, (2013), 065028.
- [29] S. Chen, Y. Li, Y. Yang, *Phys. Rev.* **D 89** (2014), 025007.
- [30] F. Canfora, F. Correa, J. Zanelli, *Phys. Rev.* **D 90**, 085002 (2014).
- [31] F. Canfora, M. Di Mauro, M. A. Kurkov, A. Naddeo, *Eur. Phys. J.* **C75** (2015) 9, 443.
- [32] E. Ayon-Beato, F. Canfora, J. Zanelli, *Phys. Lett.* **B 752**, (2016) 201-205.
- [33] F. Canfora, G. Tallarita, *Nucl. Phys.* **B 921** (2017) 394–410.
- [34] P. D. Alvarez, F. Canfora, N. Dimakis and A. Paliathanasis, *Phys. Lett.* **B 773**, (2017) 401-407.
- [35] L. Aviles, F. Canfora, N. Dimakis, D. Hidalgo, *Phys. Rev.* **D 96** (2017), 125005.
- [36] M. Shifman, "Advanced Topics in Quantum Field Theory: A Lecture Course" Cambridge University Press, (2012).
- [37] M. Shifman, A. Yung, "Supersymmetric Solitons" Cambridge University Press, (2009).